*Acta Medica Okayama*

*Volume* 47, *Issue* 6 1993 *Article* 5

DECEMBER 1993

# Astrocytic gliomas: MRI and pathological grade.

Shouji Asari* Tetsuo Makabe† Shinji Katayama‡

Takahiko Itoh** Shouhei Tsuchida††

*Okayama University,

†Okayama University,

‡Okayama Univerisity,

**Okayama University,

††Okayama University,

# Astrocytic gliomas: MRI and pathological grade.*

Shouji Asari, Tetsuo Makabe, Shinji Katayama, Takahiko Itoh, and Shouhei Tsuchida

## Abstract

The relationship between MR configuration and pathological grade was studied in 41 histologically verified supratentorial astrocytic gliomas with a 0.5T superconductive MR system. The gliomas included 13 low-grade astrocytomas (LGAs), 14 anaplastic astrocytomas (AAs) and 14 glioblastoma multiformes (GBMs). MRI configurations were classified into nine criteria which were scored and statistically analyzed. The mean values of LGAs, AAs and GBMs were 0.45 +/- 0.31, 1.18 +/- 0.20 and 1.47 +/- 0.22. In each grade, MRI score increased as pathological grades increased ($p < 0.01$-$0.001$). LGAs had significantly lower values than AAs in five of the nine criteria (55.6%); heterogeneity, cyst or necrosis, edema or mass effect, border definition, and the degree of contrast enhancement, and lower values than GBMs in eight criteria (88.9%) except for hemorrhage. Three criteria (33.3%), heterogeneity, cyst or necrosis, and flow void sign were significantly higher in GBMs than AAs. The four variables, heterogeneity, cyst or necrosis, edema or mass effect and border definition, proved to be important factors related to the pathological grade in a multiple regression analysis.

**KEYWORDS:** astocytic gliomas, pathological grade, MRI, MRI score

---

*PMID: 8128912 [PubMed - indexed for MEDLINE]

Acta Med Okayama 47 (6) 383-389 (1993)

# Astrocytic Gliomas: MRI and Pathological Grade

**Shoji Asari*, Tetsuo Makabe, Shinji Katayama, Takahiko Itoh, Shouhei Tsuchida and Takashi Ohmoto**

*Department of Neurological Surgery, Okayama University Medical School, Okayama-city 700, Japan*

**The relationship between MR configuration and pathological grade was studied in 41 histologically verified supratentorial astrocytic gliomas with a 0.5T superconductive MR system. The gliomas included 13 low-grade astrocytomas (LGAs), 14 anaplastic astrocytomas (AAs) and 14 glioblastoma multiformes (GBMs). MRI configurations were classified into nine criteria which were scored and statistically analyzed. The mean values of LGAs, AAs and GBMs were $0.45 \pm 0.31$, $1.18 \pm 0.20$, and $1.47 \pm 0.22$. In each grade, MRI score increased as pathological grades increased ($p < 0.01$-$0.001$). LGAs had significantly lower values than AAs in five of the nine criteria (55.6%); heterogeneity, cyst or necrosis, edema or mass effect, border definition, and the degree of contrast enhancement, and lower values than GBMs in eight criteria (88.9%) except for hemorrhage. Three criteria (33.3%), heterogeneity, cyst or necrosis, and flow void sign were significantly higher in GBMs than AAs. The four variables, heterogeneity, cyst or necrosis, edema or mass effect and border definition, proved to be important factors related to the pathological grade in a multiple regression analysis.**

*Key words :* **astrocytic gliomas, pathological grade, MRI, MRI score**

It is very important to predict the pathological grade of glial tumors prior to clinical management because the treatment and the prognosis of patients are dependent on accurate neuropathological diagnosis.

Ever since Damadian (1) reported prolongation of the longitudinal relaxation time (T1) and the transverse relaxation time (T2) of proton in malignant tumors using magnetic resonance (MR) imaging in 1971, and Goldsmith (2) introduced the malignancy index in gastrointestinal tumors in 1978, there have been many attempts to determine the malignancy of tumors using T1 and T2 relaxation times (3-5). But, because their values in differentiating malignant tumors from other lesions are still controversial due to the wide variation in the relaxation times, it has recently become inappropriate to predict the qualitative tumor characteristics on the basis of measurements of relaxation times alone (6-8). It is also difficult to predict the qualitative tissue characteristics from the configurations that are shown on MR images.

In this paper, the authors evaluated MR configurations of astrocytic gliomas in terms of an MRI score to determine if it could serve as a useful index for predicting the pathological grade of astrocytic gliomas.

## Materials and Methods

From March 1988 to September 1991, our department treated 41 supratentorial astrocytic glioma cases; 21 men and 20 women whose ages ranged from 5 to 77 years with the average age of 43.8 years. The tumors were graded as low-grade astrocytomas (LGAs), anaplastic astrocytomas (AAs), or glioblastoma multiformes (GBMs) based on the World Health Organization (WHO) classification of astrocytomas (9). Forty-one astrocytic gliomas consisted of 13 LGAs (6 men and 7 women, 5-72 years; average of 30.0 years), 14 AAs (8 men and 6 women, 16-77 years; average of 4.8 years), and 14 GBMs (7 men and 7 women, 30-77

* To whom correspondence should be addressed.

years; average of 54.8 years).

These tumors were histologically confirmed by means of computed tomography (CT) or MRI guided stereotactic biopsy (7 cases including 4 AAs and 3 GBMs) with 2 mm-cup biopsy forceps (Brown-Roberts-Wells system, Radionics Inc., Burlington, MA) or by surgery (34 cases including 13 LGAs, 10 AAs and 11 GBMs). In stereotactic biopsy, tumor specimens were obtained from several different parts to make an accurate diagnosis.

MR images were obtained on a 0.5 T superconducting magnet (Resona, Yokogawa Medical Systems, Tokyo, Japan) prior to biopsy or surgery in all patients. Spin echo (SE) sequences with an echo time (TE) of 25 msec and a repetition time (TR) of 600 msec were used to take T1 weighted images, and SE sequences with a long TE of 100 msec and a long TR of 2000 msec were used to take T2 weighted images. Five to ten mm slice thickness, a 256 × 256 acquisition matrix, and a 25 cm field of view were used in all studies. An axial plane image was obtained routinely and an additional coronal plane image was taken when indicated. Contrast-enhanced T1 weighted images were taken when indicated. Contrast-enhanced T1 weighted images were obtained after intravenous administration of gadolinium diethylenetriaminepentaacetic acid (Gd-DTPA) at a dose of 0.1 mmol/kg of the body weight.

The nine criteria of heterogeneity, cyst or necrosis, hemorrhage, crossing of the midline, edema or mass effect, border definition, flow void sign, and the degree and the heterogeneity of the contrast enhancement, which were modification of Dean's grading criteria (10), were scored on the basis of degree and configuration of signal abnormalities, respectively (Table 1). At first, all MR configurations were reviewed and evaluated independently by two of the authors (S. K. and T. I.) solely on the basis of the data for astrocytic gliomas. After a discussion, a score was given for each criterion. The scores were averaged for each case and for each criterion, and were subjected to statistical analysis using Student's *t*-test and a multiple regression analysis to determine the reliability of MRI score for predicting the pathological grade of astrocytic gliomas. Multiple regression analysis was performed in 7 criteria except for the contrast enhancement because it was not done in all of the cases.

**Table 1** Criteria of MR configuration and score

| MR configuration | Score |
|---|---|
| Heterogeneity | None 0, mild 1, moderate 2, marked 3 |
| Cyst or necrosis | None 0, equivocal 1, yes 2 |
| Hemorrhage | None 0, equivocal 1, yes 2 |
| Crossing of the midline | None 0, equivocal 1, yes 2 |
| Edema or mass effect | None 0, mild 1, moderate 2, severe 3 |
| Border definition | Well defined 0, poorly defined 1 |
| Flow void sign | None 0, equivocal 1, yes 2 |
| Contrast enhancement | |
| Degree | None 0, slight 1, moderate 2, marked 3 |
| Heterogeneity | None 0, homogeneous 1, heterogeneous 2 |

## Results

The astrocytic gliomas generally displayed the following MR characteristics: LGAs showed a homogeneous signal intensity, little edema or mass effect, a well-defined border with no contrast enhancement (Fig. 1); AAs showed a moderate degree of heterogeneous signal intensity, edema or mass effect and contrast enhancement, and a less-defined border (Fig. 2); GBMs showed heterogeneous signal intensity, larger edema or mass effect, a poorly defined border, and irregular and marked contrast

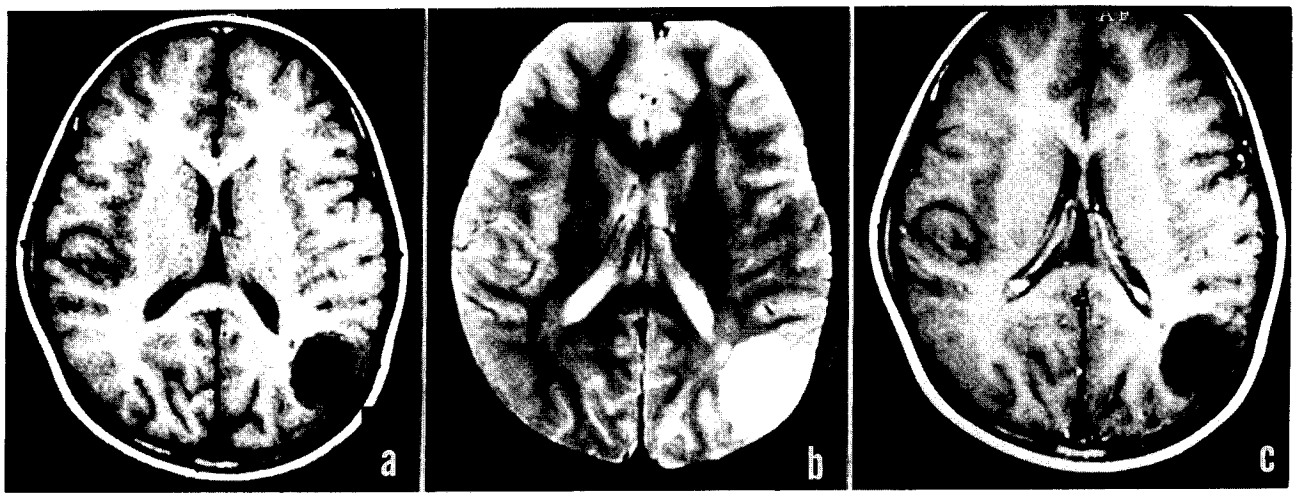


**Fig. 1** MR images of a low-grade astrocytoma showing a low-signal homogeneity, well-demarcated border, little edema, and no contrast enhancement. **(a)** T1 weighted image, **(b)** T2 weighted image, **(c)** contrast-enhanced T1 weighted image.

enhancement (Fig. 3).

The accuracy rate of diagnosis based on MR images in comparison with the histopathological results is shown in Table 2. The overall impression given by MR images was correct in 26 of 41 case (63.4 %) including 76.9 % of LGAs, 50 % of AAs and 64.3 % of GBMs.

The mean MRI score, which was the total score divided by the number of criterion in each pathological grade, was $0.45 \pm 0.31$ with a range of 0.11 to 1.0 in 13 LGAs, $1.18 \pm 0.20$ with a range of 0.78 to 1.56 in 14 AAs, and $1.47 \pm 0.22$ with a range of 0.89 to 1.89 in 14 GBMs (Table 3). The mean value of LGAs was significantly lower than those of high-grade astrocytomas including AAs and GBMs ($p < 0.001$). There was also a significant difference between AAs and GBMs ($p < 0.01$). Mean MRI score increased in proportion to the pathologi-

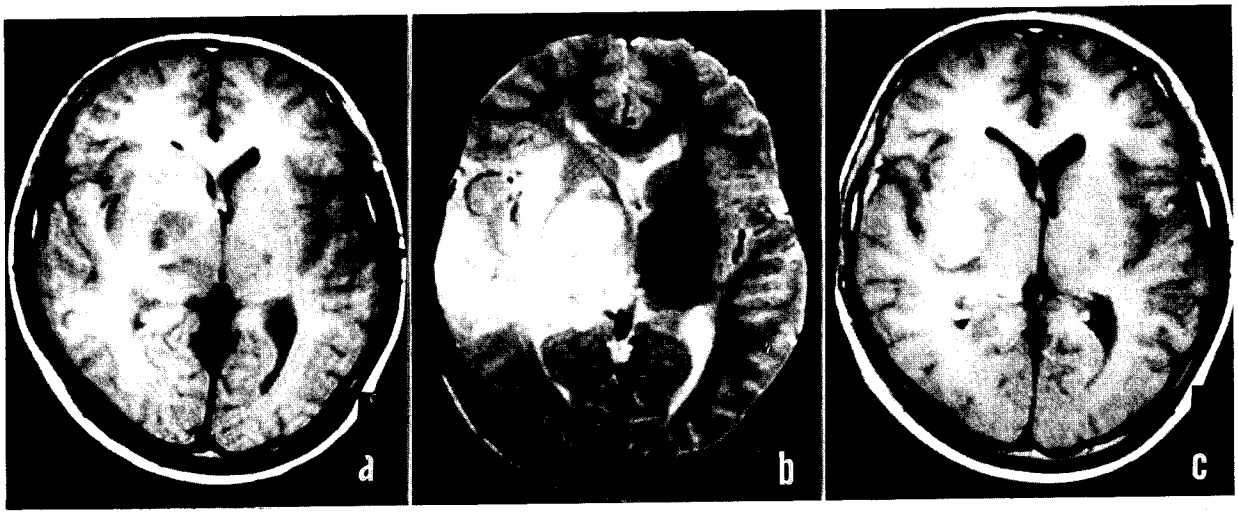


**Fig. 2** MR images of an anaplastic astrocytoma. T1 weighted image **(a)** shows a slightly heterogeneous and ill-defined low intense mass in the basal ganglia region. This mass is highly intense and accompanied by marked surrounding edema on T2 weighted image **(b)**, and well enhanced by Gd-DTPA **(c)**.

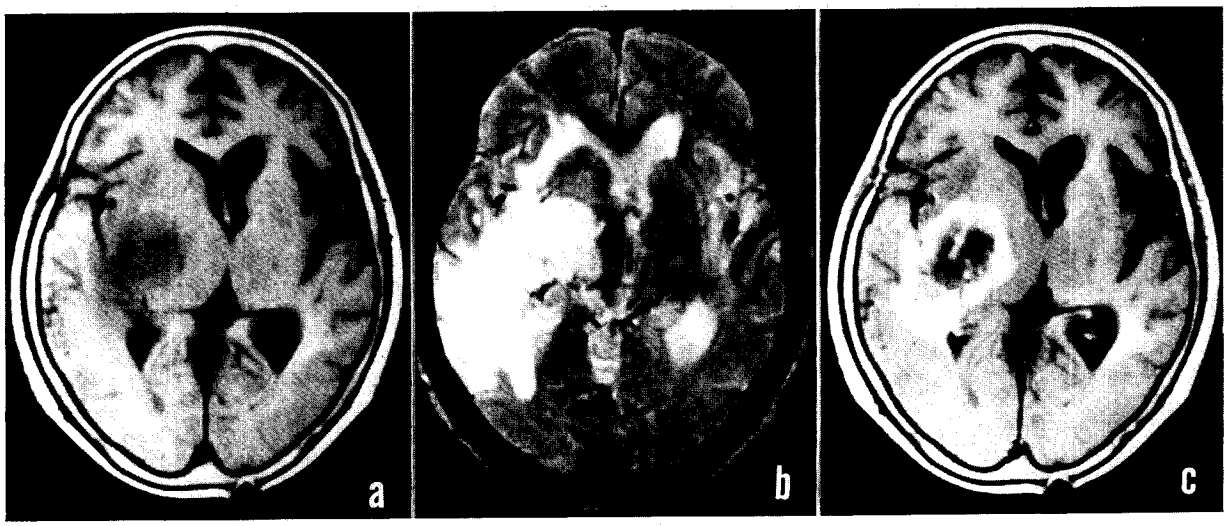


**Fig. 3** MR images of a glioblastoma multiforme. An ill-defined, low-intense mass with moderate midline shift is demonstrated in the deep temporal region on T1 weighted image **(a)**. T2 weighted image **(b)** shows a little heterogeneous high signal, poorly-defined border, and a marked edema. Contrast-enhanced T1 weighted image **(c)** demonstrates a heterogeneous, highly intense, well- but irregularly-outlined lesion which involves central low intensity indicating necrosis.

cal grade. Table 4 shows the correlation between the mean MRI score of each criterion and pathological grade.

**Table 2** Accuracy of diagnosis based on MRI diagnosis to histopathological results

| MRI diagnosis | Histopathological results | | | Total |
|---|---|---|---|---|
| | LGAs | AAs | GBMs | |
| LGAs | 10 | 2 | 1 | 13 |
| AAs | 3 | 7 | 4 | 14 |
| GBMs | 0 | 5 | 9 | 14 |
| Total | 13 | 14 | 14 | 41 |

LGAs = low-grade astrocytomas
AAs = anaplastic astrocytomas
GBMs = glioblastoma multiformes

**Table 3** Correlation between the MRI score of all cases and pathological grade

| Pathological grade | Mean MRI score |
|---|---|
| Low-grade astrocytomas | 0.45±0.31 |
| Anaplastic astrocytomas | 1.18±0.20 * |
| Glioblastoma multiformes | 1.47±0.22 +, § |

* $p<0.01$, compared to low-grade astrocytomas
+ $p<0.01$, compared to anaplastic astrocytomas
§ $p<0.001$, compared to low-grade astrocytomas

Five of 9 criteria (55.6 %) revealed statistically significant lower values in LGAs than in AAs. These criteria included edema or mass effect, border definition and the degree of contrast enhancement ($p < 0.001$), heterogeneity ($p < 0.01$), and cyst or necrosis ($p < 0.05$). There were significant differences between LGAs and GBMs in 8 of the 9 criteria (88.9 %); heterogeneity, cyst or necrosis, edema or mass effect, border definition and the degree of contrast enhancement ($p < 0.001$), and crossing of the midline, flow void sign and heterogeneity by contrast enhancement ($p < 0.05$). Although MRI scores of GBMs revealed higher values in all criteria than AAs, only 3 criteria were statistically significant; heterogeneity, cyst or necrosis, and flow void sign ($p < 0.05$). Hemorrhage was not seen in LGAs, but it was observed in one case of AA (7.1 %) and one case of GBM (7.1 %). Crossing of the midline was not seen in LGAs, but it was seen in 4 AAs (28.6 %) and 5 GBMs (35.7 %) (Fig. 4). Flow void sign was noticed in 4 GBMs (28.6 %) on T2 weighted images (Fig. 5).

Multiple regression analysis was formulated for the prediction of tumor grade for this study (Table 5):

$$Y = 0.612275 + 0.205964(HET) + 0.1986(CN) + 0.0393738(HEM) + 0.140996(CM) + 0.267088(EM) + 0.325206(BD) + 0.234188(FV),$$

where HET = heterogeneity, CN = cyst or necrosis,

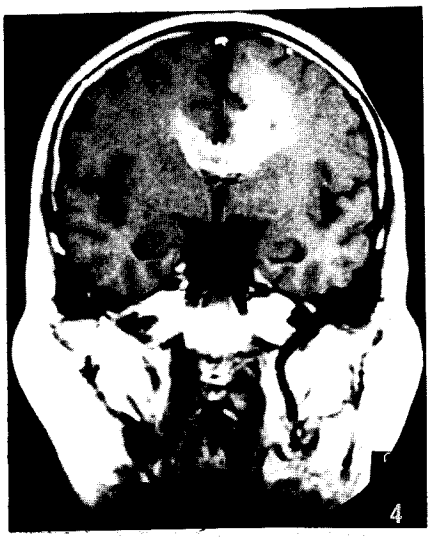


Fig. 4

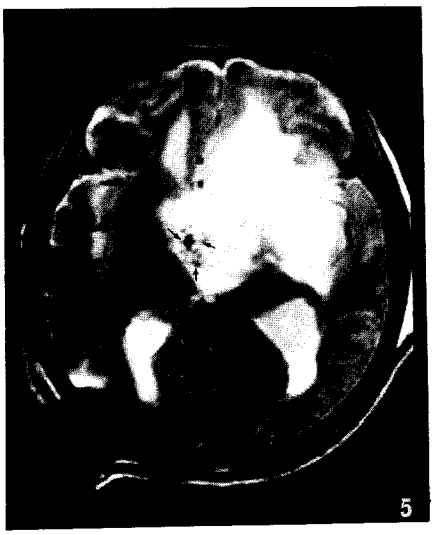


Fig. 5

**Fig. 4** Contrast-enhanced T1 weighted image, coronal plane, of glioblastoma multiforme shows the so-called "the buttertfly" shaped configuration.
**Fig. 5** T2 weighted image of glioblstoma multiforme reveals the ill-defined, high-intense lesion which partly involves low-intense spots (arrows), so-called "flow void sign", indicating abnormal tumor vessels.

**Table 4** Correlation between MRI score of each criterion and pathological grade

| | Heterogeneity | Cyst or necrosis | Hemorrhage | Crossing of midline | Edema or mass effect | Border definition | Flow void sign | Contrast enhancement | |
|---|---|---|---|---|---|---|---|---|---|
| | | | | | | | | Degree | Heterogeneity |
| LGAs | 0.62 ±0.65 | 0.69 ±0.85 | 0 | 0 | 1.0 ±0.58 | 0.23 ±0.44 | 0 | 0.8 ±0.79 | 1.0 ±0.94 |
| AAs | 1.71 ±0.47 | 1.36 ±0.63 | 0.28 ±0.73 | 0.36 ±0.63 | 2.07 ±0.73 | 1.07 ±0.27 | 0 | 2.20 ±0.63 | 1.7 ±0.48 |
| GBMs | 2.14 ±0.53 | 1.79 ±0.41 | 0.28 ±0.73 | 0.64 ±0.93 | 2.36 ±0.74 | 1.0 ±0.39 | 0.57 ±0.94 | 2.67 ±0.65 | 2.0 |

LGAs = low-grade astrocytomas, AAs = anaplastic astrocytomas, GBMs = glioblastoma multiformes,
Values are expressed as mean value ± standard deviation, * = $p < 0.05$, + = $p < 0.01$, § = $p < 0.001$

**Table 5** Statistical data given by multiple regression analysis

| MR configuration | Standard regression coefficient | *P* value | Correlation coefficient |
|---|---|---|---|
| Heterogeneity | 0.499703 | < 0.001 | 0.742246 |
| Cyst or necrosis | 0.358715 | < 0.001 | 0.572233 |
| Hemorrhage | 0.092801 | N. S. | 0.192791 |
| Crossing of the midline | 0.211184 | < 0.02 | 0.380266 |
| Edema or mass effect | 0.443189 | < 0.001 | 0.620354 |
| Border definition | 0.249256 | < 0.001 | 0.592607 |
| Flow void sign | 0.190363 | < 0.02 | 0.395468 |

N. S.: not significant

HEM = hemorrhage, CM = crossing of the midline, EM = edema or mass effect, BD = border definition, and FV = flow void sign.

As a result, four variables, indicating heterogeneity, cyst or necrosis, edema or mass effect, and border definition, were found to be statistically significant predictors for distinguishing pathological grade.

## Discussion

Because of the low measurement value of T1 and T2 relaxation times in determining the qualitative tumor characteristics (6–8), we attempted to evaluate the pathological grade of astrocytic glioma series by scoring each MR configuration. Dean *et al.* (10) described seven criteria including crossing of the midline, edema, heterogeneity, hemorrhage, border definition, cyst or necrosis, and mass effect for evaluation of the pathological grade of astrocytomas on MR images in 1990. However, they did not include flow void sign and the effect on MR findings after contrast enhancement which were very important factors for histopathological diagnosis of the tumors. So, we added these factors and proposed a new MR grading criteria in this study.

The mean values of all cases and criteria were lower in LGAs than in AAs and GBMs. By statistical analysis, the mean value was significantly lower in five criteria of LGAs than in AAs and lower than GBMs in eight criteria. These facts indicate that it is possible to easily differentiate LGAs from high-grade astrocytomas (AAs and GBMs) on MR images. Also in accuracy rate based on MR findings to histopathological results, the diagnosis of LGAs were made correctly in high percentage rather than in AAs and GBMs. Sometimes, however, there is a difficulty in distinguishing of the pathological grade only by means of MR findings (Fig. 6). The mean values of all criteria of AAs were lower than those of GBMs, and in the three criteria of heterogeneity, cyst or necrosis, and flow void sign, the differences were statistically significant. According to multiple regression analysis, four variables were determined to be statistically significant predictors for tumor malignancy: heterogeneity, cyst or necrosis, edema or mass effect and border definition. Also, the heterogeneous tissue components including cystic or necrotic degeneration, hemorrhage, abnormal tumor vessels or increasing density of viable cells may be responsible for the pathological grade (11–13) and complicate the signal intensity and configuration on MR images (14). Between AAs and GBMs, some configurations overlapped each other. This fact seemed to decrease the accuracy rate of MR diagnosis between AAs and GBMs. However, the different degree

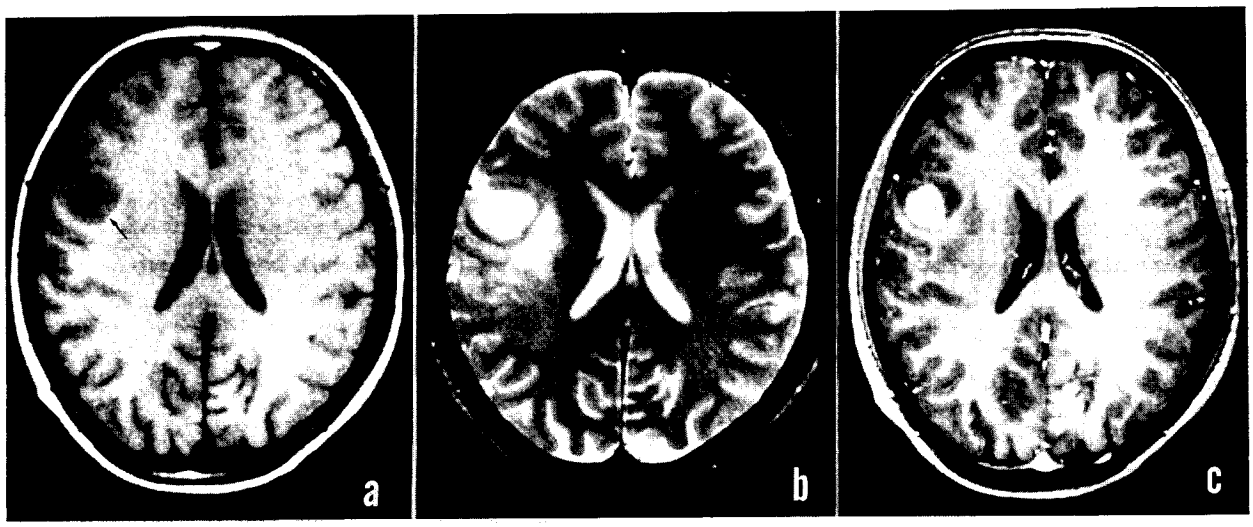


**Fig. 6** One case showing atypical MR images of glioblastoma multiforme. A well-defined, round, slightly low-intense mass is shown on T1 weighted image (**a**, arrow), and T2 weighted image (**b**) reveals a round and high-intense lesion with little edema. This lesion is slightly enhanced by Gd-DTPA administration (**c**). MRI score of this case is 0.89. Although MR images of this tumor resembled those of low-grade astrocytoma, histopathological diagnosis was glioblastoma multiforme.

of the necrotic or cystic foci and increased abnormal vascularity seemed to be the key criteria in distinguishing GBMs from AAs. Also from a histological view point, the presence of necrosis is the most important factor in distinguishing them (11, 13).

There was a significant difference in the values for edema or mass effect between LGAs and high-grade astrocytomas (AAs and GBMs), but no significant difference between AAs and GBMs. This result indicates that edema may result not only from the density of tumor cells in the surrounding area, but also from the differences in the degree of spreading of vasogenic edema (15, 16).

Concerning the border definition of tumors, it was well-demarcated in LGAs, but unclear in high-grade astrocytomas (AAs and GBMs). Statistical analysis showed a significant difference between these two groups.

Extensive or microhemorrhages are sometimes observed in gliomas of all grades (17). In our series, the incidence of hemorrhage was not statistically significant different among the pathological grades. Kondziolka *et al.* (18) reported that the incidence of hemorrhage was 12.5 % in LGAs and 19 % in GBMs. It seems unlikely that the hemorrhage is closely related to the pathological grade of gliomas.

It is well known that GBMs sometimes cross the midline through the corpus callosum and appears as "the butterfly" pattern. Although this phenomenon was valuable in differentiating pathological grades of gliomas in Dean's report (10), there was no statistically significant difference between AAs and GBMs in our series. This discrepancy may result from the location of the tumor, as some tumors were in the deep structures of the hemisphere and infiltrated through the midline into the contralateral site in our AAs group.

The degree of contrast enhancement is shown to be closely related to the pathological grade of astrocytic gliomas. Graif *et al.* (19) showed a mean decrease of 16 % in T1 relaxation time in LGAs and that of 29 % in high-grade astrocytomas in the maximal contrast enhancement region. The heterogeneity of signal intensity after contrast enhancement also depends on the tumor malignancy. This may be due to the various damages of the blood-brain barrier and the complexity of the tumor tissue including necrosis, cyst, hemorrhage, abnormal tumor vessels and/or viable tumor cells.

Evaluation of the pathological grade using MRI score is so simple and practical that we believe MRI score can serve to predict the qualitative tumor characteristics prior to clinical management. An additional advantage of this method is the applicability to different kinds of MRI machines because there is no need to calculate relaxation times.

Acknowledgments. We would like to thank Katsuzo Kunishio, M, D.

from our department for his help with statistical analysis, and Mr. Hideki Wakimoto, Mrs. Yoshiko Ohmori and Miss Yumiko Mizukawa for the preparation of the figures and manuscript.

## References

1. Damadian R: Tumor detection by nuclear magnetic resonance. Science (1971) **171**, 1151-1153.
2. Goldsmith M, Koutcher J and Damadian R: Application of the NMR malignancy index to human gastro-intestinal tumors. Cancer (1978) **41**, 183-191.
3. Araki T, Inouye T, Suzuki H, Machida T and Iio M: Magnetic resonance imaging of brain tumors: Measurement of T1. Radiology (1984) **150**, 95-98.
4. Englund E, Brun A, Larsson EM, Gyorffy-Wagner Z and Persson B: Tumors of the central nervous system: Proton magnetic relaxation times T1 and T2 and histopathological correlates. Acta Radiol Diagn (1986) **27**, 653-659.
5. Just M and Thelen M: Tissue characterization with T1, T2 and proton density values: Results in 160 patients with brain tumors. Radiology (1988) **169**, 779-785.
6. Brady TJ, Buonanno FS, Pykett IL, New PFJ, Davis KR, Pohost GM and Kistler JP: Preliminary clinical results of proton ($^1$H) imaging of cranial neoplasms: *In vivo* measurements of T1 and mobile proton density. Am J Neuroradiol (1983) **4**, 225-228.
7. Komiyama M, Yagura H, Baba M, Yasui T, Hakuba A, Nishimura S and Inoue Y: MR imaging: Possibility of tissue characterization of brain tumors using T1 and T2 values. Am J Neuroradiol (1987) **8**, 65-70.
8. Lee BCP, Kneeland JB, Cahill PT and Deck MDF: MR recognition of supratentorial tumors. Am J Neuroradiol (1985) **6**, 871-878.
9. Zülch KJ: Histological typing of tumours of the central nervous system; in International Histological Classification of Tumours, No. 21, WHO, Geneva (1979).
10. Dean BL, Drayer BP, Bird CR, Flom RA, Hodak JA, Coons SW and Carey RG: Gliomas: Classification with MR imaging. Radiology (1990) **174**, 411-415.
11. Burger PC: Malignant astrocytic neoplasms: Classification, pathologic anatomy, and response to therapy. Simen Oncol (1986) **13**, 16-20.
12. Cohadon F, Aouad N, Rougier A, Vital C, Rivel J and Dartigues JF: Histologic and non-histologic factors correlated with survival time in supratentorial astrocytic tumors. J Neurooncol (1985) **3**. 105-111.
13. Nelson JS, Tsukada Y, Schoenfeld D, Fulling K, Lamarche J and Peress N: Necrosis as a prognostic criterion in malignant supratentorial, astrocytic gliomas. Cancer (1983) **52**, 550-554.
14. Price AC, Runge VM, Allen JH, Partain CL and James AE Jr: Primary glioma: Diagnosis with magnetic resonance imaging. J Comput Tomogr (1986) **10**, 325-334.
15. Johnson PC, Hunt SJ and Drayer BP: Human cerebral gliomas: Correlation of postmortem MR imaging and neuropathologic findings. Radiology (1989) **170**, 211-217.
16. Laster DW, Ball MR, Moody DM, Witcofski RL and Kelly DL Jr: Results of nuclear magnetic resonance with cerebral glioma: Comparison with computed tomography. Surg Neurol (1984) **22**, 113-122.
17. Wakai S, Yamakawa K, Manaka S and Takakura K: Spontaneous intracranial hemorrhage caused by brain tumor: Its incidence and clinical significance. Neurosurgery (1982) **10**, 437-444.
18. Kondziolka D, Bernstein M, Resch L, Tator CH, Fleming JFR, Vanderlinden RG and Schutz H: Significance of hemorrhage into brain tumors: Clinicopathological study. J Neurosurg (1987) **57**, 852-857.
19. Graif M, Bydder GM, Steiner RE, Niendorf P, Thomas DGT and Young IR: Contrast-enhanced MR imaging of malignant brain tumors. Am J Neuroradiol (1985) **6**, 855-862.

Received April 28, 1993; accepted August 2, 1993.